(Standard Project Submission Form) の提出を行った。*In silico* スクリーニングを含む QSAR に関して、OECD では QSAR 系の検証を実施しないという方針が出され、本年度より VMG-NA では本体においては議論を行わず、QSAR ワーキンググループを設置して情報交換を行うことになった。本年度は、VMG-NA5 にあわせて行われたアドオンミーティーングにおいて解析結果の報告を行い、今後の共同研究も含めた方針について議論を行った。内分泌かく乱物質の評価基準やガイドライン策定は、国際的な強調のもとに行われるべきであり、早期の問題解決に向けて我が国においても今後も研究を進める必要があると考察された。

E. 結論

本研究班でこれまで構築及び検証を進めてきた各スクリーニング系より得られたデータの比較解析の結果、それぞれ特徴の異なる *in silico*、*in vitro* 及び *cell free* 系でのスクリーニング手法の組み合わせにより、内分泌かく乱の可能性のある化学物質について効率的かつ信頼性の高い優先順位付けが可能となることが示された。今後、内分泌かく乱の標的となりうる他の核内受容体についても各手法の構築を進める必要がある。一方、本研究班で構築を進めたパスウェイスクリーニングは、標的の不明な化学物質について受容体作用の評価が可能であり、さらなるデータの充実を図ることにより生体影響をより詳細に検討可能な手法として有用性が期待される。

内分泌かく乱化学物質の問題解決に向けた取り組みや評価基準やガイドライン策定は、国際的な強調のもとに行われるべきである。本研究班における個別のスクリーニング系についての研究成果及び比較解析結果については、これまで OECD において報告を行ってきた。本研究班で検討を進めてきたレポーター遺伝子測定系のうち ERα 系、AR 系についてガイドライン化に向けた提案を行っており、今後も引き続き国際的な議論への対応が必要である。

F. 研究発表

1. 誌上発表

なし

2. 学会発表

菅野 純、内分泌かく乱化学物質問題研究の現状・問題点、及び今後の展開 化学物質の環境リスクに関する国際シンポジウム 化学物質の内分泌かく乱作用について～10年間のあゆみ～ 2007 年 12 月 9-10 日、さいたま

G. 知的財産所有権の出願・登録状況(予定も含む)

1. 特許取得

なし

2. 実用新案登録

なし

3. その他

なし

表1　各レポーター遺伝子測定系において測定済み化合物数

NR	Host cell	Assay system		No. of compounds
ERalpha	HeLa	stable	agonist assay	350
			antagonist assay	350
		transient	agonist assay	240
ERbeta	HeLa	transient	agonist assay	340
AR	CHO-K1	stable	agonist assay	200
			antagonist assay	200
TRbeta*	CHO-K1	transient	agonist assay	200
			antagonist assay	200

* TRbeta / RXR co-transfected CHO cell was used for assay

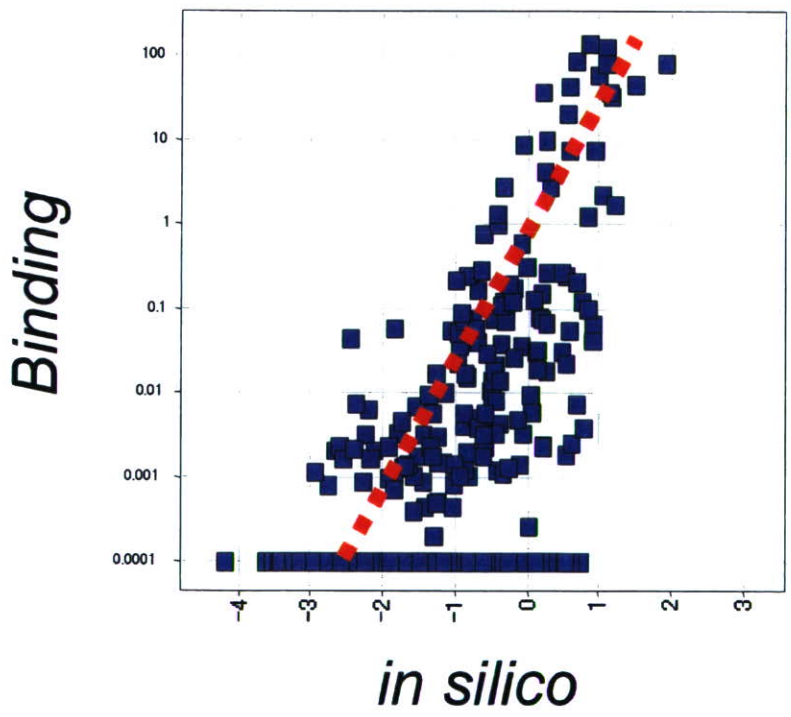

図1　*in silico*結合予測値と実測値の比較

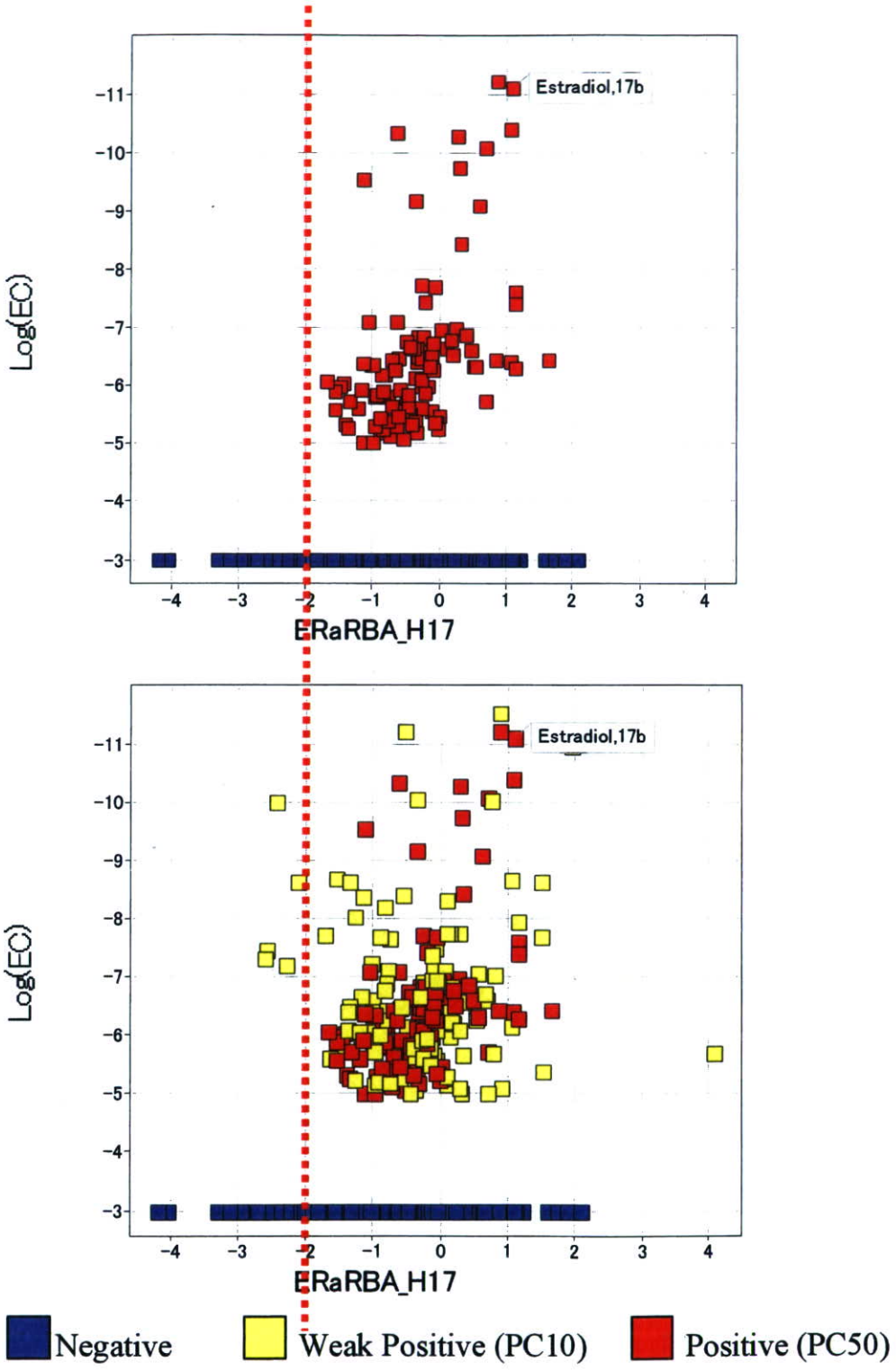

図2　*in silico*結合予測値とレポーターアッセイによる活性値の比較

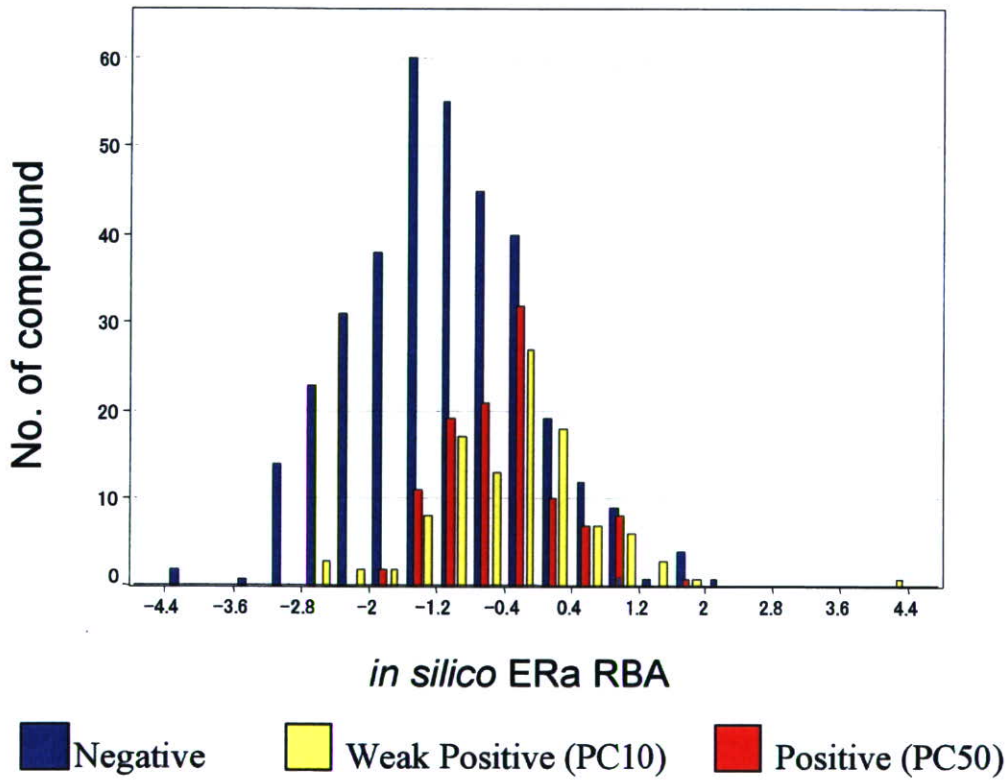

図3　*in silico*結合予測値に対するレポーターアッセイ結果の化合物数分布

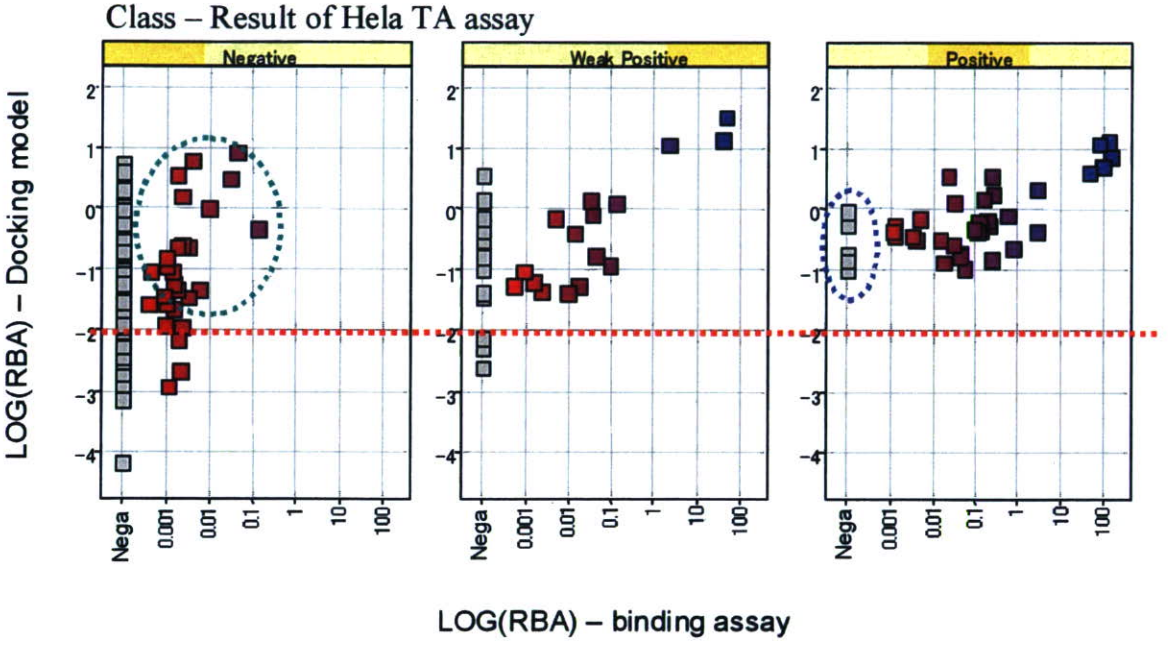

図4　レポーター活性測定結果ごとの*in silico*結合予測値と結合実測値

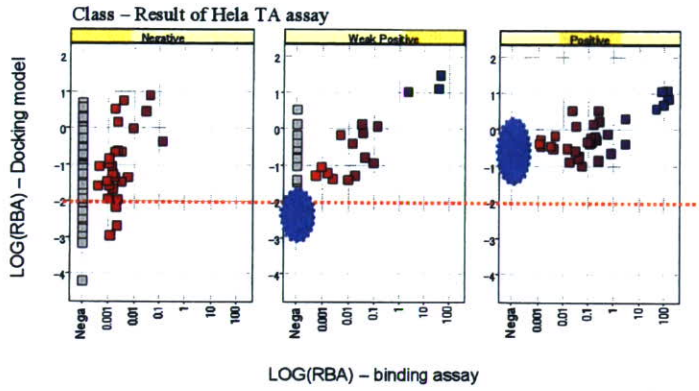

左図の青枠の化合物の測定結果

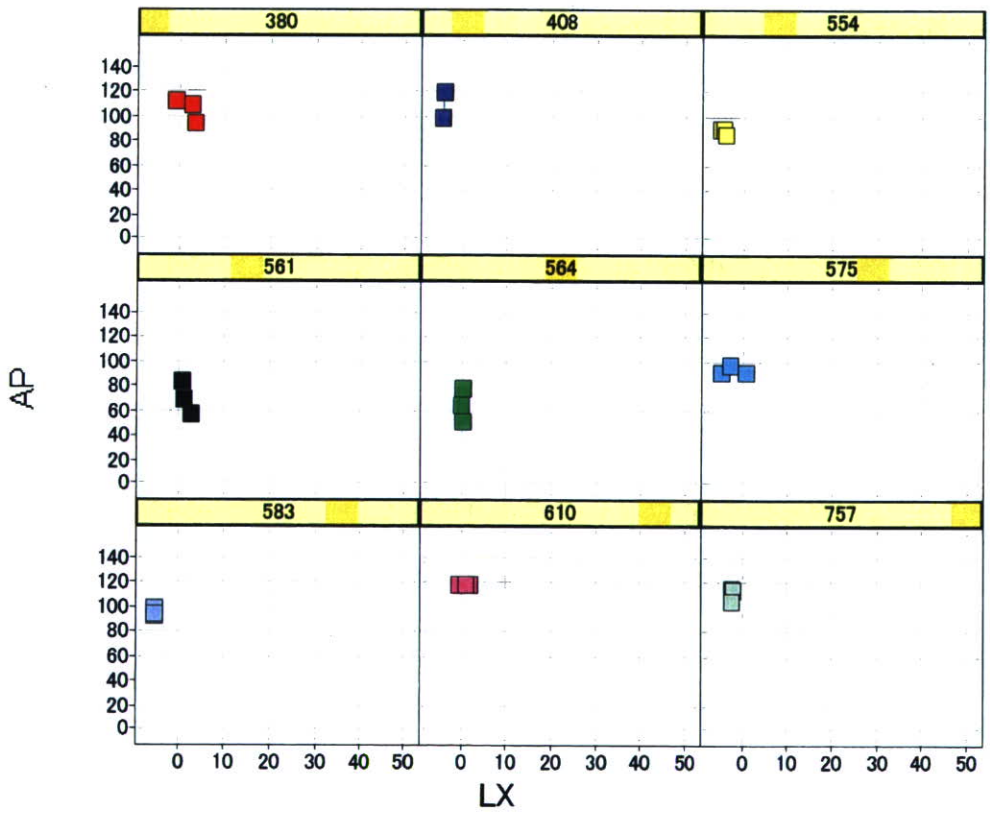

図5 レポーター活性測定と結合測定の結果が一致しない化合物の受容体共役因子スクリーニング結果1

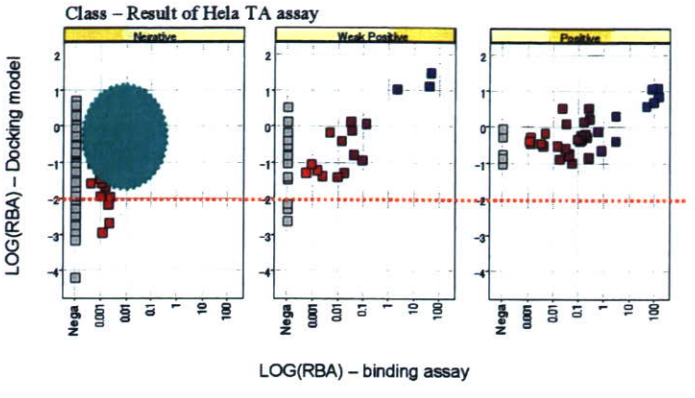

左図の緑枠の化合物の測定結果

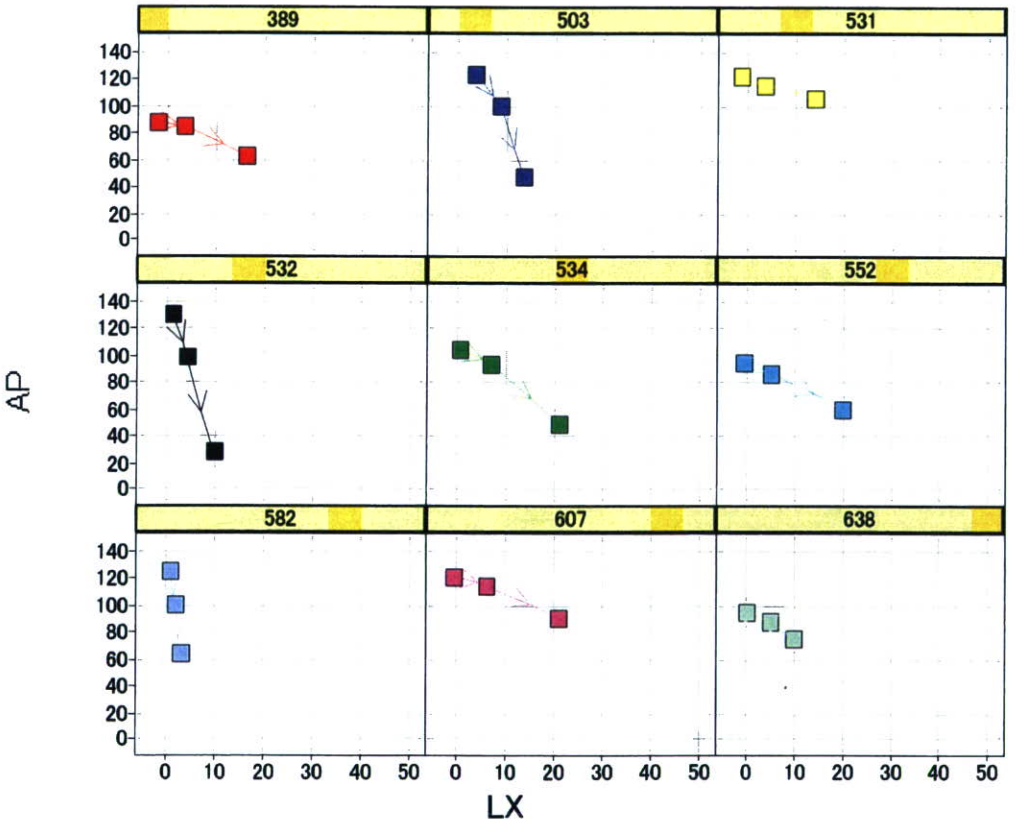

図6 レポーター活性測定と結合測定の結果が一致しない化合物の受容体共役因子スクリーニング結果2

別添5

研究成果の刊行に関する一覧表レイアウト

書籍

著者氏名	論文タイトル名	書籍全体の編集者名	書 籍 名	出版社名	出版地	出版年	ページ
水澤博、小原有弘、増井徹	バイオ研究の舞台裏－細胞バンクと研究倫理－		ポピュラーサイエンス282	裳華房		2007	

雑誌

発表者氏名	論文タイトル名	発表誌名	巻名	ページ	出版年
Kiyosawa N, Uehara T, Gao W, Omura K, Hirode M, Shimizu T, Mizukawa Y, Ono A, Miyagishima T, Nagao T, and Urushidani T	Identification of glutathione depletion-responsive genes using phorone-treated rat liver	J Toxicol Sci	32(5)	469 - 486	2007
Omura K, Kiyosawa N, Uehara T, Hirode M, Shimizu T, Miyagishima T, Ono A, Nagao T, and Urushidani T	Gene expression profiling of methapyrilene-induced hepatotoxicity in rat	J Toxicol Sci	32(4)	387 - 399	2007
Uehara T, Kiyosawa N, Hirode M, Omura K, Shimizu T, Ono A, Mizukawa Y, Miyagishima T, Nagao T, and Urushidani T	Gene expression profiling of methapyrilene-induced hepatotoxicity in rat	J Toxicol Sci	33(1)	37 - 50	2008
Takeuchi M, Takeuchi K, Kohara A, Satoh M, Shioda S, Ozawa Y, et al	Chromosomal instability in human mesenchymal stem cells immortalized with human papilloma virus E6, E7, and hTERT genes	In Vitro Cell Dev Biol Anim	43 (3-4)	129 - 138	2007
Ono K., Satoh M., Yoshida T., Ozawa Y., Kohara A., Takeuchi M., Mizusawa H., Sawada H.	Species identification of animal cells by nested PCR targeted to mitochondrial DNA	In Vitro Cell Dev Biol Anim	43	168 - 175	2007
水谷実穂、板井昭子	論理的分子設計に基づく創薬	バイオテクノロジージャーナル	7(2)	247 - 250	2007
水谷実穂、板井昭子	分子構造から考える薬物の作用機序(2) 論理的分子設計からの創薬	医薬ジャーナル	No.3	5-10	2007
武藤進、水谷実穂、板井昭子	蛋白構造と論理的分子設計に基づく創薬	Medical Science Digest	33(10)	1057 - 1060	2007
小原有弘，水澤博	JCRB 細胞バンク:厚生労働省	細胞工学	26(10)	1177-8	2007
水澤博、小原有弘、増井徹	わが国におけるヒト研究資源バンクの現状と今後	医学のあゆみ	222(2)	113	2007
小原有弘、大谷梓、小澤裕、塩田節子、増井徹、水澤博	培養細胞研究資源のマイコプラズマ汚染調査	Tiss.Cult.Res. Commun.	26	159 -163	2007
水澤博、増井徹、竹内昌男、小原有弘	-190C 気相式液体窒素細胞保存システム	Tiss.Cult.Res. Commun.	26	165 -170	2007
水澤博，小澤裕，小原有弘，増井徹，佐藤元信，岩瀬秀，深海薫，西條薫，中村幸夫	培養細胞で頻発するクロスコンタミネーションへの警戒(印刷中)	実験医学			2008

裳華房　ポピュラー・サイエンス　282

バイオ研究の舞台裏

――細胞バンクと研究倫理――

水澤　博・小原有弘・増井　徹　共著

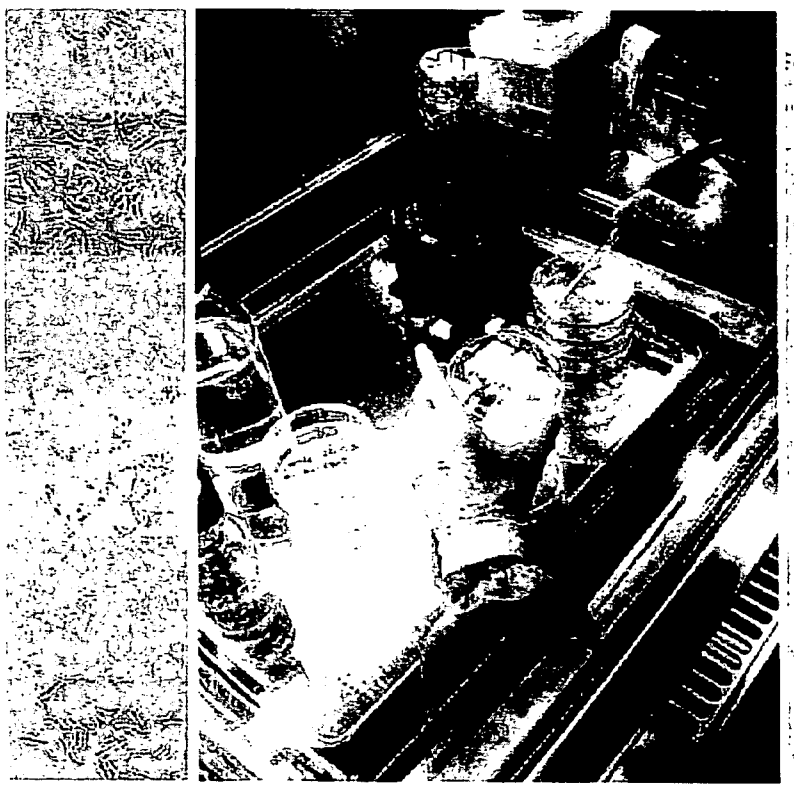

ポピュラーサイエンス 282
バイオ研究の舞台裏 細胞バンクと研究倫理
水澤 博
小原有弘
増井 徹 共著
裳華房

9784785387822
ISBN978-4-7853-8782-2
C0045 ¥1600E
1920045016004
定価（本体1600円＋税）

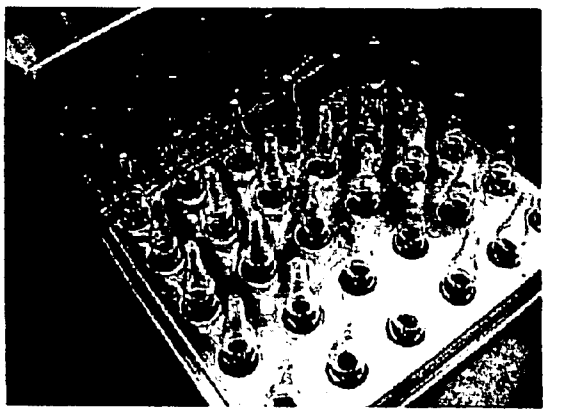

SHOKABO

The Journal of Toxicological Sciences,
Vol.32, No.5, 469-486, 2007

IDENTIFICATION OF GLUTATHIONE DEPLETION-RESPONSIVE GENES USING PHORONE-TREATED RAT LIVER

Naoki KIYOSAWA[1], Takeki UEHARA[1], Weihua GAO[1], Ko OMURA[1], Mitsuhiro HIRODE[1], Toshinobu SHIMIZU[1], Yumiko MIZUKAWA[1,2], Atsushi ONO[1], Toshikazu MIYAGISHIMA[1], Taku NAGAO[3] and Tetsuro URUSHIDANI[1,2]

[1]*Toxicogenomics Project, National Institute of Biomedical Innovation, 7-6-8 Asagi, Ibaraki, Osaka 567-0085, Japan*

[2]*Department of Pathophysiology, Faculty of Pharmaceutical Sciences, Doshisha Women's College of Liberal Arts, Kodo, Kyotanabe, Kyoto 610-0395, Japan*

[3]*National Institute of Health Sciences, 1-18-1 Kamiyoga, Setagaya-Ku, Tokyo 158-8501, Japan*

(Received August 17, 2007; Accepted August 27, 2007)

ABSTRACT — To identify candidate biomarker gene sets to evaluate the potential risk of chemical-induced glutathione depletion in livers, we conducted microarray analysis on rat livers administered with phorone (40, 120 and 400 mg/kg), a prototypical glutathione depletor. Hepatic glutathione content was measured and glutathione depletion-responsive gene probe sets (GSH probe sets) were identified using Affymetrix Rat Genome 230 2.0 GeneChip by the following procedure. First, probe sets, whose signal values were inversely correlated with hepatic glutathione content throughout the experimental period, were statistically identified. Next, probe sets, whose average signal values were greater than 1.5-fold compared to those of controls 3 hr after phorone treatment, were selected. Finally, probe sets without unique Entrez Gene ID were removed, ending up with 161 probe sets in total. The usefulness of the identified GSH probe sets was verified by a toxicogenomics database. It was shown that signal profiles of the GSH probe sets in rats treated with bromobenzene were strongly altered compared with other chemicals. Focusing on bromobenzene, time-course profiles of hepatic glutathione content and gene expression revealed that the change in gene expression profile was marked after the bromobenzene treatment, whereas hepatic glutathione content had recovered after initial acute depletion, suggesting that the gene expression profile did not reflect the hepatic glutathione content itself, but rather reflects a perturbation of glutathione homeostasis. The identified GSH probe sets would be useful for detecting glutathione-depleting risk of chemicals from microarray data.

KEY WORDS: Glutathione, Rat, Liver, Microarray, Toxicity, Toxicogenomics, Phorone

INTRODUCTION

Microarray analysis displays tens of thousands of nucleotide probes on a substrate surface, and enables the measurement of mRNA levels of large numbers of genes simultaneously (Rockett and Dix, 2000). Microarray analysis is aimed at toxicological investigation and is called toxicogenomics (Boverhof and Zacharewski, 2006). This is thought to be useful for such points as: I) understanding the molecular mechanisms of toxicity, II) the early prediction of drug toxicity risk, and III) improvement in extrapolation of experimental animal data to humans (Orphanides, 2003). At present, the liver is one of the most favored target organs in Toxicogenomics studies for the following reasons: 1) it is exposed to relatively higher levels of administered drugs, 2) it is a relatively homogenous organ and thus easy to sample, and 3) it can dramatically affect the pharmaco/toxico-kinetics of the drugs in the body by the first-pass effect (Parkinson, 2001). Furthermore, hepatotoxicity has been a critical concern in drug development (Kaplowitz, 2004; Li, 2002).

Correspondence: Tetsuro URUSHIDANI (E-mail: turushid@dwc.doshisha.ac.jp)

These issues have motivated toxicologists to investigate liver toxicity using the toxicogenomics technique.

The Toxicogenomics Project in Japan (TGP; http://wwwtgp.nibio.go.jp/index-e.html) has been completed by the National Institute of Health Sciences and 17 pharmaceutical companies after 5 years' collaboration from 2002 (Urushidani and Nagao, 2005; Takashima *et al.*, 2006). In the project, five rats per group were administered with toxicological prototype drugs once daily, where three dose-ranges were set, and liver samples were collected 3, 6, 9 and 24 hr after a single treatment, as well as 4, 9, 15 and 29 days after repetitive treatment. Of the collected liver samples, three samples per group were subjected to microarray analysis using the Affymetrix GeneChip system. In addition, toxicological data, such as blood chemistry and histopathology, were collected simultaneously. Such a large-scale database would be invaluable for scientists not only as a reference database but also as a resource for screening candidate toxicogenomic biomarker sets.

Glutathione serves vital functions in detoxifying electrophiles and scavenging free radicals (Lu, 1999), and hepatotoxicity caused by glutathione depletion has been intensely investigated. In the case of acetaminophen overdosage, acetaminophen is metabolically activated by phase I drug metabolizing enzymes to form a reactive metabolite, *N*-acetyl-*p*-benzoquinone imine (NAPQI), which covalently binds to proteins (Dahlin *et al.*, 1984; James *et al.*, 2003). Although NAPQI can be detoxified by glutathione conjugation under ordinary conditions, an excess dose of acetaminophen depletes 90% of hepatic glutathione, and reactive NAPQI forms protein adducts (Mitchell *et al.*, 1973; James *et al.*, 2003), resulting in hepatocyte necrosis.

Previously, sixty-nine gene probe sets of Rat Genome U34A GeneChip (Affymetrix, Inc.) were identified as glutathione depletion-responsive genes, using L-buthionine-(S,R)-sulfoximine (BSO) as a glutathione-depleting agent (Kiyosawa *et al.*, 2004). Although the probe sets were thought to be useful for evaluation of drug-induced glutathione deficiency in rat liver, the study had two major drawbacks. First, the sample size used for the study was relatively small: one dose setting and one time point of observation, using 4 rats per group. Secondly, BSO depletes hepatic glutathione by inhibiting γ-glutamylcysteine synthetase, a key enzyme of glutathione synthesis (Moinova and Mulcahy, 1999). In the case of acetaminophen-induced glutathione depletion, an overdose of acetaminophen depletes hepatic glutathione by extended conjugation of glutathione with activated metabolites such as NAPQI. Therefore, BSO-induced glutathione depletion would probably not appropriately reflect the drug-induced one. For these reasons, an alternative glutathione-depleting model, other than the BSO model, would be useful for better explaining drug-induced glutathione depletion, in view of the gene expression profile.

Phorone is an α, β-unsaturated compound, which strongly depletes hepatic glutathione content by conjugation with glutathione, by action of glutathione *S*-transferase (GST), and is excreted from liver (Boyland and Chasseaud, 1967; van Doorn *et al.*, 1978). Comparing the glutathione-depleting mechanism of phorone with that of BSO, the phorone-induced glutathione depletion mechanism is thought to be more similar to that induced by acetaminophen overdosing, where activated metabolites such as NAPQI deplete glutathione by being conjugated with glutathione and then are excreted from liver.

In this paper, we present candidate biomarker probe sets of RAE 230A GeneChip for evaluation of the potential risk of drug-induced glutathione depletion in rat livers, using phorone as a glutathione-depleting agent. The toxicological significance of identified biomarker probe sets was examined using a large-scale TGP database.

MATERIALS AND METHODS

Chemicals

Phorone, acetaminophen, thioacetamide, phenylbutazone, glibenclamide, methapyrilene hydrochloride and perhexiline maleate were purchased from Sigma-Aldrich (St. Louis, MO, USA). Clofibrate, aspirin and chlorpromazine were purchased from Wako Pure Chemical Industries (Osaka, Japan). Bromobenzene, hexachlorobenzene, carbon tetrachloride and coumarin were purchased from Tokyo Chemical Industry (Tokyo, Japan).

Animal treatment

Six-week old-male Crj:CD(SD)IGS rats (Charles River Japan, Kanagawa, Japan) were used in the study. The animals were individually housed in stainless-steel cages in a room that was lighted for 12 hr (7:00-19:00) daily, ventilated with an air-exchange rate of 15 times per hour, and maintained at 21-25°C with a relative humidity of 40-70%. Each animal was allowed free access to water and pellet food (CRF-1, sterilized by

radiation, Oriental Yeast Co., Japan). Five rats per group were administered with phorone (40, 120 or 400 mg/kg, i.p.). Five rats per group were administered orally with acetaminophen (1000 mg/kg), bromobenzene (300 mg/kg), clofibrate (300 mg/kg), chlorpromazine (45 mg/kg), glibenclamide (1000 mg/kg), methapyrilene (100 mg/kg), phenylbutazone (200 mg/kg), aspirin (450 mg/kg), carbon tetrachloride (300 mg/kg), coumarin (150 mg/kg), hexachlorobenzene (300 mg/kg), perhexiline maleate (150 mg/kg) or thioacetamide (45 mg/kg). Blood samples were collected in tubes containing heparin lithium 3, 6, 9, or 24 hr after treatment for biochemical assay. The animals were then euthanized and the liver was removed and soaked in RNA*later* (Ambion, Austin, TX, USA) immediately after sampling and stored at −80°C until use for gene expression analysis. In the animals treated with phorone or bromobenzene, another aliquot of liver sample was immediately frozen in liquid nitrogen for measurement of hepatic glutathione contents. The remaining liver samples were then removed and fixed in 10% neutral buffered formalin for histopathological examination. The experimental protocol was reviewed and approved by the Ethics Review Committee for Animal Experimentation of the National Institute of Health Sciences.

Plasma biochemistry

Activities of alanine aminotransferase (ALT) and aspartate aminotransferase (AST) in plasma were determined using a 7080 Clinical Analyzer (Hitachi High-Technologies Corporation, Tokyo, Japan).

Histopathology

The fixed samples were dehydrated through graded alcohols and embedded in paraffin. Serial sections 2-3 μm thick were stained with hematoxylin and eosin for pathological examination.

Measurement of hepatic glutathione content

The liver samples (0.1 g) were homogenized with 5% 5-sulfosalicylic acid (Sigma-Aldrich) and centrifuged at 12,000 rpm for 10 min at 4°C. The supernatant was used for the measurement of total glutathione content in the liver using the Total Glutathione Quantification Kit (Dojindo Laboratories), according to the manufacturer's instructions.

Microarray analysis

Liver samples were homogenized with RLT buffer, supplied in the RNeasy Mini Kit (Qiagen, Valencia, CA, USA), using Mill Mixer (Qiagen) and zirconium beads. Total RNA was isolated using Bio Robot 3000 (Qiagen). DNase I treatment was performed using RNase-Free DNase set (Qiagen) for 15 min at room temperature. GeneChip analysis was performed on 3 out of 5 samples in each group according to the Affymetrix standard protocol. Briefly, a total of RNA of 5 μg prepared from the individual rat liver samples was used for cDNA synthesis using the T7-$(dT)_{24}$ primer (Affymetrix) and Superscript Choice System (Invitrogen, Carlsbad, CA, USA). The cDNA was purified using cDNA Cleanup Module (Affymetrix), and biotin-labeled cRNA mix was transcribed using the BioArray High Yield RNA Transcription Labeling Kit (Enzo Diagnostics, Farmingdale, NY, USA). Ten micrograms of fragmented cRNA cocktails were hybridized to the RAE 230A GeneChip array for all samples except for that of phorone- and corresponding vehicle-treated rats, which were hybridized to the RAE 230 2.0 array for 18 hr at 45°C at 60 rpm. GeneChip was washed and stained using Fluidics Station 400 (Affymetrix) according to the Affymetrix standard protocol and scanned using Gene Array Scanner (Affymetrix). The scanned data images were digitalized using Affymetrix Microarray Suite ver. 5.0 (Affymetrix), and the data was scaled by adjusting the mean Signal value to 500.

Microarray data analysis

We primarily use gloval mean normalization for data analysis in our project. Firstly, using vehicle- and phorone (40 and 120 mg/kg)-treated rats, where the total number of rats was 36, both Spearman's and Pearson's correlation coefficients between the signal value and hepatic glutathione content were calculated for all the probe sets that existed on the RAE 230A array. The probe sets with both Spearman's coefficients and Pearson's coefficients less than -0.329 were chosen as statistically significant inverse correlations ($N=36$, $p < 0.05$). Secondly, probe sets, whose average signal values in 120 mg/kg phorone-treated rats at 3 h were above 1.5 compared to those of corresponding controls were selected. Then, probe sets, whose detection calls determined by Microarray Suite ver. 5.0 were all present 3 hr after phorone treatment, were selected. Finally, annotation for each probe set was obtained using NetAffx Website (Liu *et al.*, 2003), and probe sets without unique Entrez Gene ID were excluded from the analysis. For each probe set, the signal data was z-score normalized in the vehicle- and phorone (40, 120 and 400 mg/kg)-treated group. All the z-score

normalized signal data were presented as a heat map and z-score normalized glutathione content data was also presented as a heat map.

Statistical analysis

Dunnett's test was performed for serum chemistry and glutathione content data (between phorone-treated rat groups and vehicle-treated group at the same time point), using R software (www.r-project.org). Serum chemistry data (other than that of phorone-treated rats) was analyzed by F-test to evaluate the homogeneity of variance. If the variance was homogeneous, Student's *t*-test was applied. If the variance was heterogeneous, Aspin-Welch's *t*-test was performed (Snedecor and Cochran, 1989). F-test, Student's *t*-test and Aspin-Welch's *t*-test were performed using Microsoft Excel 2007. Both Spearman's and Pearson's correlation coefficients were calculated using Microsoft Excel 2007. A p-value of < 0.05 was considered statistically significant. Principal component analysis (PCA) was performed using the Spotfire Functional Genomics Package ver. 17.4.832 (Spotfire, Somerville, MA, USA).

RESULTS

Plasma biochemistry in phorone-treated rats

There were no apparent fluctuations of plasma ALT activity in 40 and 120 mg/kg phorone-treated rats throughout the experimental period (Fig. 1). Plasma ALT activity was obviously elevated in rats 24 hr after 400 mg/kg phorone treatment.

Glutathione content in phorone-treated rat liver

Hepatic glutathione content was significantly decreased 3, 6 and 9 hr for 40 mg/kg phorone-treated rats, and recovered above the control level 24 hr after treatment (Fig. 2). Hepatic glutathione content was significantly decreased to an 8.3-fold lower level compared with the control 3 hr after the 120 mg/kg phorone-treated rats, and gradually recovered 6 and 9 hr after treatment, resulting in a 1.52-fold higher level compared with control 24 hr after treatment. Hepatic glutathione content was significantly decreased to a 22- to 30-fold lower level compared with control 3, 6 and 9 hr after the 400 mg/kg phorone-treated rats, and recovered to the control level 24 hr after treatment.

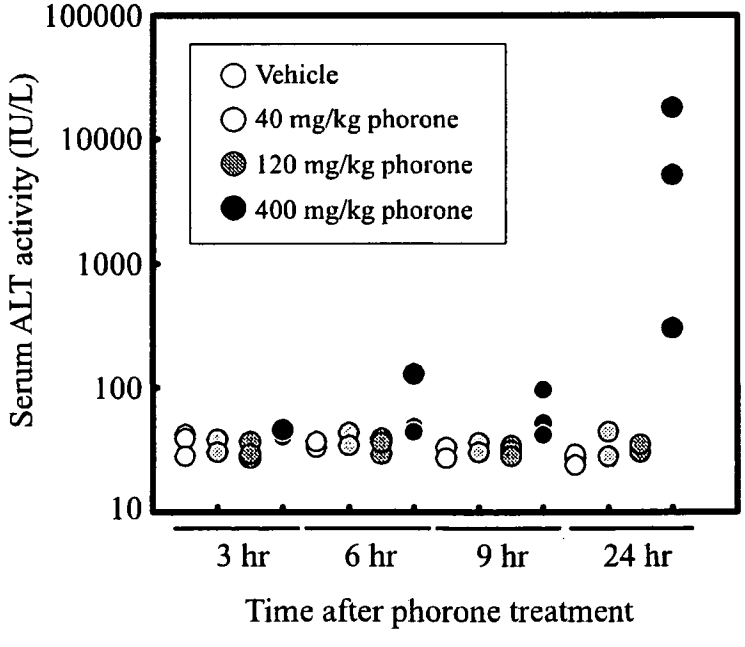

Fig. 1. Activity of alanine aminotransferase in plasma. Each dot represents the value of an individual animal.

Identification of glutathione deficiency-correlated gene probe sets

A hundred and sixty-one probe sets were identified as glutathione deficiency-correlated gene probe sets, or GSH probe sets (Table 1), and classified to 5 groups, i.e., "antioxidant, phase II drug metabolizing enzymes, and oxidative stress markers" (11 probe sets), "transporter" (13 probe sets), "metabolism" (20 probe sets), "transcription factors and signal transduction-related, and protein turnover-related genes" (79 probe sets), and "miscellaneous" (37 probe sets). Both the z-score transformed hepatic glutathione content and z-score transformed signal levels of the GSH probe sets are presented as a heat map (Fig. 3). PCR primers and TaqMan probes for 4 genes from the list above, namely tribbles homolog 3 (accession no. AB020967), heme oxygenase-1 (NM_012580), thioredoxin reductase-1 (NM_031614) and γ-glutamylcysteine synthetase modifier subunit (NM_017305), were synthesized and quantitative RT-PCR was performed using the TaqMan Universal PCR Master Mix (Applied Biosystems), and the mRNA level was quantified with a GeneAmp 5700 Sequence Detection System (Applied Biosystems) according to the manufacturer's instructions. It was confirmed that quantification by GeneChip was sufficient (data not shown).

Plasma biochemistry and histopathological findings in rat liver treated with various hepatotoxicants

Rats treated with bromobenzene, methapyrilene or thioacetamide showed significant increase in plasma ALT activity 24 hr after treatment (Table 2). Rats treated with acetaminophen, chlorpromazine, glibenclamide or methapyrilene showed significant increase in serum AST activity 24 hr after treatment. Rats treated with acetaminophen, bromobenzene, methapyrilene, carbon tetrachloride, coumarin or thioacetamide showed histopathological changes 24 hr after treatment, while rats treated with clofibrate, chlorpromazine, glibenclamide, phenylbutazone, aspirin,

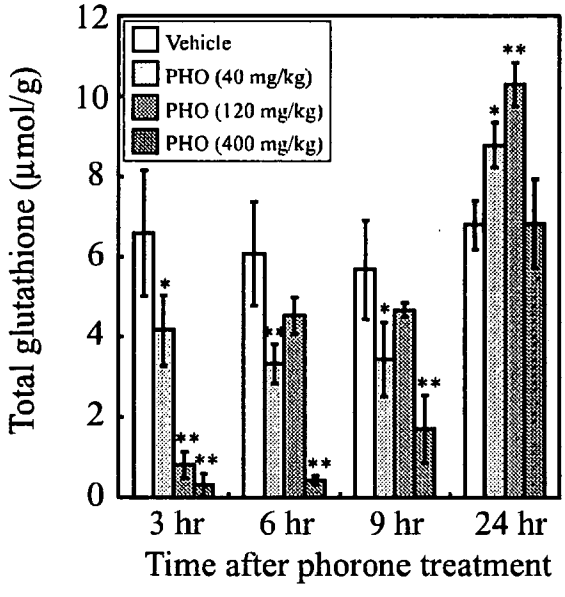

Fig. 2. Hepatic glutathione content after phorone treatment.
Three rats per group were treated with 40, 120 or 400 mg/kg phorone or vehicle, and the livers were removed 3, 6, 9 and 24 hr after treatment. Hepatic glutathione content (total) was measured and the data are presented as mean ± S.D. ** and *, $p<0.01$ and $p<0.05$ by Dunnett's test, respectively.

Table 1. Glutathione depletion-responsive gene probe sets (GSH probe sets).

Affymetrix probe ID	Correlation coefficient		Gene Symbol	Annotation
	Spearman's	Pearson's		
Antioxidant, phase II drug-metabolizing enzymes and oxidative stress markers				
1368037_at	−0.602	−0.368	Cbr1	carbonyl reductase 1
1387221_at	−0.720	−0.712	Gch	GTP cyclohydrolase 1
1368503_at	−0.702	−0.650	Gch	GTP cyclohydrolase 1
1370030_at	−0.570	−0.448	Gclm	glutamate cysteine ligase, modifier subunit
1370080_at	−0.611	−0.609	Hmox1	heme oxygenase (decycling) 1
1387282_at	−0.680	−0.589	Hspb8	heat shock 22kDa protein 8
1388721_at	−0.747	−0.660	Hspb8	heat shock 22kDa protein 8
1389578_at	−0.649	−0.582	Isrip	ischemia/reperfusion inducible protein
1372510_at	−0.589	−0.578	Srxn1	Sulfiredoxin 1 homolog (S. cerevisiae)
1398791_at	−0.600	−0.471	Txnrd1	thioredoxin reductase 1
1386958_at	−0.666	−0.459	Txnrd1	thioredoxin reductase 1
Transporter				
1374423_at	−0.711	−0.688	Hiat1_predicted	hippocampus abundant gene transcript 1 (predicted)
1370934_at	−0.656	−0.579	Nup153	nucleoporin 153
1367803_at	−0.430	−0.523	Nup54	nucleoporin 54
1371754_at	−0.330	−0.497	Slc25a25	solute carrier family 25 (mitochondrial carrier, phosphate carrier), member 25
1369099_at	−0.356	−0.567	Slc30a1	solute carrier family 30 (zinc transporter), member 1
1370286_at	−0.858	−0.813	Slc38a2	solute carrier family 38, member 2
1398771_at	−0.651	−0.520	Slc3a2	solute carrier family 3 (activators of dibasic and neutral amino acid transport), member 2
1387130_at	−0.726	−0.455	Slc40a1	solute carrier family 39 (iron-regulated transporter), member 1
1387693_a_at	−0.731	−0.601	Slc6a9	solute carrier family 6 (neurotransmitter transporter, glycine), member 9
1369772_at	−0.609	−0.473	Slc6a9	solute carrier family 6 (neurotransmitter transporter, glycine), member 9
1373787_at	−0.619	−0.513	Slc6a9	solute carrier family 6 (neurotransmitter transporter, glycine), member 9
1368391_at	−0.780	−0.700	Slc7a1	solute carrier family 7 (cationic amino acid transporter, y^+ system), member 1
1368392_at	−0.591	−0.626	Slc7a1	solute carrier family 7 (cationic amino acid transporter, y^+ system), member 1
Metabolism				
1387925_at	−0.747	−0.574	Asns	asparagine synthetase
1386928_at	−0.352	−0.409	Bcat2	branched chain aminotransferase 2, mitochondrial
1374034_at	−0.762	−0.756	Cars_predicted	cysteinyl-tRNA synthetase (predicted)
1368709_at	−0.537	−0.492	Fut1	fucosyltransferase 1
1375852_at	−0.441	−0.532	Hmgcr	3-hydroxy-3-methylglutaryl-Coenzyme A reductase
1387848_at	−0.413	−0.500	Hmgcr	3-hydroxy-3-methylglutaryl-Coenzyme A reductase
1376418_a_at	−0.679	−0.549	Iars_predicted	isoleucine-tRNA synthetase (predicted)

Table 1. Continued.

Affymetrix probe ID	Correlation coefficient		Gene Symbol	Annotation
	Spearman's	Pearson's		
1389551_at	–0.373	–0.359	Lactb2	lactamase, beta 2
1371350_at	–0.773	–0.683	LOC683283	similar to S-adenosylmethionine synthetase isoform type-2 (Methionine adenosyltransferase 2) (AdoMet synthetase 2) (Methionine adenosyltransferase II) (MAT-II)
1377287_at	–0.495	–0.532	Mars2_predicted	methionine-tRNA synthetase 2 (mitochondrial) (predicted)
1375684_at	–0.554	–0.490	Neu1	neuraminidase 1
1367811_at	–0.675	–0.459	Phgdh	3-phosphoglycerate dehydrogenase
1369785_at	–0.754	–0.691	Ppat	phosphoribosyl pyrophosphate amidotransferase
1388756_at	–0.614	–0.529	Ppcs	phosphopantothenoylcysteine synthetase
1372665_at	–0.682	–0.633	Psat1	phosphoserine aminotransferase 1
1375964_at	–0.641	–0.615	Psph	phosphoserine phosphatase
1388521_at	–0.428	–0.544	Pycs_predicted	pyrroline-5-carboxylate synthetase (glutamate gamma-semialdehyde synthetase) (predicted)
1372602_at	–0.490	–0.460	RGD1311800	similar to genethonin 1
1398452_at	–0.421	–0.431	RGD1559923_predicted	similar to chromosome 14 open reading frame 35 (predicted)
1372009_at	–0.569	–0.478	Yars	tyrosyl-tRNA synthetase
Transcription factor, signal transduction-related and protein turnover-related gene				
1388179_at	–0.370	–0.379	Acvr2b	activin receptor IIB
1369146_a_at	–0.433	–0.479	Ahr	aryl hydrocarbon receptor
1378140_at	–0.600	–0.606	Arl11	ADP-ribosylation factor-like 11
1367960_at	–0.470	–0.485	Arl4a	ADP-ribosylation factor-like 4A
1389623_at	–0.605	–0.623	Atf1	activating transcription factor 1
1375941_at	–0.594	–0.513	Baiap2l1	BAI1-associated protein 2-like 1
1374947_at	–0.584	–0.567	Bcar3_predicted	breast cancer anti-estrogen resistance 3 (predicted)
1376754_at	–0.771	–0.740	Cars_predicted	cysteinyl-tRNA synthetase (predicted)
1391572_at	–0.804	–0.802	Cars_predicted	cysteinyl-tRNA synthetase (predicted)
1387087_at	–0.720	–0.734	Cebpb	CCAAT/enhancer binding protein (C/EBP), beta
1387244_at	–0.504	–0.371	Cgrrf1	cell growth regulator with ring finger domain 1
1372498_at	–0.626	–0.608	Ciapin1	cytokine induced apoptosis inhibitor 1
1399141_at	–0.640	–0.664	Clk4	CDC like kinase 4
1376811_a_at	–0.571	–0.534	Cpsf6_predicted	cleavage and polyadenylation specific factor 6, 68kDa (predicted)
1369737_at	–0.558	–0.614	Crem	cAMP responsive element modulator
1370979_at	–0.433	–0.475	Ddx20	DEAD/H (Asp-Glu-Ala-Asp/His) box polypeptide 20, 103kD
1375901_at	–0.497	–0.360	Ddx21a	DEAD (Asp-Glu-Ala-Asp) box polypeptide 21a
1373200_at	–0.581	–0.505	Eef1e1_predicted	eukaryotic translation elongation factor 1 epsilon 1 (predicted)

Table 1. Continued.

Affymetrix probe ID	Correlation coefficient		Gene Symbol	Annotation
	Spearman's	Pearson's		
1368967_at	−0.629	−0.484	Eif2b3	eukaryotic translation initiation factor 2B, subunit 3 gamma
1386888_at	−0.794	−0.776	Eif4ebp1	eukaryotic translation initiation factor 4E binding protein 1
1388666_at	−0.581	−0.588	Encl	ectodermal-neural cortex 1
1382059_at	−0.593	−0.634	Fbxo30	F-box protein 30
1372526_at	−0.675	−0.776	Flcn	folliculin
1374530_at	−0.671	−0.601	Fzd7_predicted	frizzled homolog 7 (Drosophila) (predicted)
1373499_at	−0.731	−0.622	Gas5	growth arrest specific 5
1388953_at	−0.682	−0.665	Gnl3	guanine nucleotide binding protein-like 3 (nucleolar)
1373094_at	−0.788	−0.587	Gtf2h1_predicted	general transcription factor II H, polypeptide 1 (predicted)
1367741_at	−0.618	−0.579	Herpud1	homocysteine-inducible, endoplasmic reticulum stress-inducible, ubiquitin-like domain member 1
1372693_at	−0.462	−0.559	Hnrpa1	heterogeneous nuclear ribonucleoprotein A1
1387430_at	−0.754	−0.774	Hsf2	heat shock factor 2
1388587_at	−0.571	−0.636	Ier3	immediate early response 3
1367795_at	−0.666	−0.597	Ifrd1	interferon-related developmental regulator 1
1368160_at	−0.644	−0.700	Igfbp1	insulin-like growth factor binding protein 1
1387440_at	−0.432	−0.330	Ireb2	iron responsive element binding protein 2
1373374_at	−0.813	−0.812	Lmo4	LIM domain only 4
1373303_at	−0.339	−0.409	LOC312030	similar to splicing factor, arginine/serine-rich 2, interacting protein
1374154_at	−0.762	−0.677	LOC312030	Similar to splicing factor, arginine/serine-rich 2, interacting protein
1374857_at	−0.555	−0.445	LOC499709	similar to nucleolar protein family A, member 1
1373133_at	−0.630	−0.692	LOC500282	similar to ADP-ribosylation factor-like 10C
1368874_a_at	−0.775	−0.801	Mafg	v-maf musculoaponeurotic fibrosarcoma oncogene family, protein G (avian)
1368273_at	−0.342	−0.453	Mapk6	mitogen-activated protein kinase 6
1384427_at	−0.766	−0.764	Mdm2_predicted	transformed mouse 3T3 cell double minute 2 homolog (mouse) (predicted)
1388990_at	−0.544	−0.492	Mki67ip	Mki67 (FHA domain) interacting nucleolar phosphoprotein
1375442_at	−0.670	−0.696	Mphosph10_predicted	M-phase phosphoprotein 10 (U3 small nucleolar ribonucleoprotein) (predicted)
1368308_at	−0.513	−0.622	Myc	myelocytomatosis viral oncogene homolog (avian)
1374437_at	−0.717	−0.665	Nars	asparaginyl-tRNA synthetase
1376704_a_at	−0.577	−0.485	Ndnl2	necdin-like 2
1389996_at	−0.645	−0.657	Nek1_predicted	NIMA (never in mitosis gene a)-related expressed kinase 1 (predicted)
1389765_at	−0.564	−0.579	Nle1_predicted	notchless homolog 1 (Drosophila) (predicted)
1368173_at	−0.444	−0.403	Nol5	nucleolar protein 5
1368032_at	−0.451	−0.365	Nolc1	nucleolar and coiled-body phosphoprotein 1
1387152_at	−0.375	−0.508	Nrbf2	nuclear receptor binding factor 2

Table 1. Continued.

Affymetrix probe ID	Correlation coefficient		Gene Symbol	Annotation
	Spearman's	Pearson's		
1368068_a_at	–0.605	–0.488	Pacsin2	protein kinase C and casein kinase substrate in neurons 2
1372857_at	–0.720	–0.706	Pacsin2	protein kinase C and casein kinase substrate in neurons 2
1374326_at	–0.576	–0.544	Ppan	peter pan homolog (Drosophila)
1369104_at	–0.618	–0.554	Prkaa1	protein kinase, AMP-activated, alpha 1 catalytic subunit
1368087_a_at	–0.419	–0.407	Ptpn21	protein tyrosine phosphatase, non-receptor type 21
1371081_at	–0.740	–0.765	Rapgef4	Rap guanine nucleotide exchange factor (GEF) 4
1374750_at	–0.773	–0.799	Rapgef6_predicted	Rap guanine nucleotide exchange factor (GEF) 6 (predicted)
1388522_at	–0.689	–0.713	RGD1310383_predicted	similar to T-cell activation protein phosphatase 2C (predicted)
1374945_at	–0.587	–0.463	RGD1359191	GCD14/PCMT domain containing protein RGD1359191
1373075_at	–0.762	–0.664	RGD1560888_predicted	similar to Cell division protein kinase 8 (Protein kinase K35) (predicted)
1372062_at	–0.703	–0.708	RGD1563395_predicted	similar to cyclin-dependent kinase 2-interacting protein (predicted)
1371517_at	–0.660	–0.627	RGD1566234_predicted	similar to Grb10 protein (predicted)
1377503_at	–0.558	–0.606	Riok2	RIO kinase 2 (yeast)
1387201_at	–0.766	–0.774	Rnf138	ring finger protein 138
1389258_at	–0.592	–0.653	Rnf138	ring finger protein 138
1376440_at	–0.741	–0.715	Rnf139_predicted	ring finger protein 139 (predicted)
1398572_at	–0.670	–0.547	Rnmt	RNA (guanine-7-) methyltransferase
1376065_at	–0.662	–0.617	Rrs1_predicted	RRS1 ribosome biogenesis regulator homolog (S. cerevisiae) (predicted)
1375441_at	–0.724	–0.680	Sars1	seryl-aminoacyl-tRNA synthetase 1
1374864_at	–0.370	–0.339	Spry2	sprouty homolog 2 (Drosophila)
1388967_at	–0.744	–0.714	Tcfe3_predicted	transcription factor E3 (predicted)
1388780_at	–0.683	–0.681	Terf2ip	telomeric repeat binding factor 2, interacting protein
1387450_at	–0.695	–0.708	Tgfa	transforming growth factor alpha
1370694_at	–0.858	–0.760	Trib3	tribbles homolog 3 (Drosophila)
1386321_s_at	–0.835	–0.676	Trib3	tribbles homolog 3 (Drosophila)
1370695_s_at	–0.831	–0.701	Trib3	tribbles homolog 3 (Drosophila)
1388868_at	–0.779	–0.736	Zfp216_predicted	zinc finger protein 216 (predicted)
Miscellaneous				
1385616_a_at	–0.734	–0.557	Asf1a_predicted	ASF1 anti-silencing function 1 homolog A (S. cerevisiae) (predicted)
1389569_at	–0.647	–0.578	Bxdc2	brix domain containing 2
1373196_at	–0.378	–0.414	Efha2	EF hand domain family, member A2
1372873_at	–0.599	–0.673	Fbxo38_predicted	F-box protein 38 (predicted)
1373836_at	–0.412	–0.503	Fyttd1	Forty-two-three domain containing 1
1374043_at	–0.379	–0.444	Gramd3	GRAM domain containing 3

Table 1. Continued.

Affymetrix probe ID	Correlation coefficient		Gene Symbol	Annotation
	Spearman's	Pearson's		
1390208_at	–0.586	–0.522	Htatip2_predicted	HIV-1 tat interactive protein 2, homolog (human) (predicted)
1371995_at	–0.802	–0.762	Klhl21_predicted	kelch-like 21 (Drosophila) (predicted)
1374879_x_at	–0.525	–0.490	Larp5_predicted	La ribonucleoprotein domain family, member 5 (predicted)
1388709_at	–0.683	–0.558	LOC362703	similar to WD-repeat protein 43
1384101_at	–0.682	–0.722	LOC682507	similar to Neural Wiskott-Aldrich syndrome protein (N-WASP)
1373761_at	–0.530	–0.535	LOC686611	similar to Protein FAM60A (Tera protein)
1373282_at	–0.596	–0.503	LOC686808	similar to mitochondrial carrier protein MGC4399
1372869_at	–0.554	–0.510	LOC689842	similar to Nucleolar GTP-binding protein 1 (Chronic renal failure gene protein) (GTP-binding protein NGB)
1373904_at	–0.749	–0.702	Lysmd2_predicted	LysM, putative peptidoglycan-binding, domain containing 2 (predicted)
1393239_at	–0.349	–0.462	Mtfr1_predicted	Mitochondrial fission regulator 1 (predicted)
1387950_at	–0.644	–0.629	Nip7	nuclear import 7 homolog (S. cerevisiae)
1373445_at	–0.732	–0.645	Nol8_predicted	nucleolar protein 8 (predicted)
1373737_at	–0.664	–0.674	ORF19	open reading frame 19
1376118_at	–0.603	–0.543	Otub2_predicted	OTU domain, ubiquitin aldehyde binding 2 (predicted)
1374438_at	–0.447	–0.460	Otud4	OTU domain containing 4
1374612_at	–0.669	–0.585	Papd5_predicted	PAP associated domain containing 5 (predicted)
1388355_at	–0.751	–0.650	Rbm17	RNA binding motif protein 17
1389065_at	–0.458	–0.498	Rbm34	RNA binding motif protein 34
1389228_at	–0.685	–0.607	RGD1304825_predicted	similar to RIKEN cDNA 2010309E21 (predicted)
1372185_at	–0.621	–0.634	RGD1306582	similar to RIKEN cDNA 2610205E22
1390392_at	–0.754	–0.718	RGD1309602_predicted	similar to RIKEN cDNA 2500001K11 (predicted)
1372329_at	–0.657	–0.627	RGD1311435	similar to hypothetical protein PRO0971
1373049_at	–0.492	–0.490	RGD1562136_predicted	similar to D1Ertd622e protein (predicted)
1388900_at	–0.719	–0.671	RGD1566118_predicted	RGD1566118 (predicted)
1372871_at	–0.717	–0.711	RGD735175	hypothetical protein MGC:72616
1375565_at	–0.513	–0.518	Timm22	translocase of inner mitochondrial membrane 22 homolog (yeast)
1390237_at	–0.573	–0.351	Timm8a	translocase of inner mitochondrial membrane 8 homolog a (yeast)
1373277_at	–0.624	–0.577	Tm2d3_predicted	TM2 domain containing 3 (predicted)
1374793_at	–0.518	–0.522	Wdr3_predicted	WD repeat domain 3 (predicted)
1371729_at	–0.473	–0.544	Ypel5	yippee-like 5 (Drosophila)
1390476_at	–0.740	–0.680	Zbtb39_predicted	Zinc finger and BTB domain containing 39 (predicted)
1373767_at	–0.634	–0.552	Zfand2a	zinc finger, AN1-type domain 2A

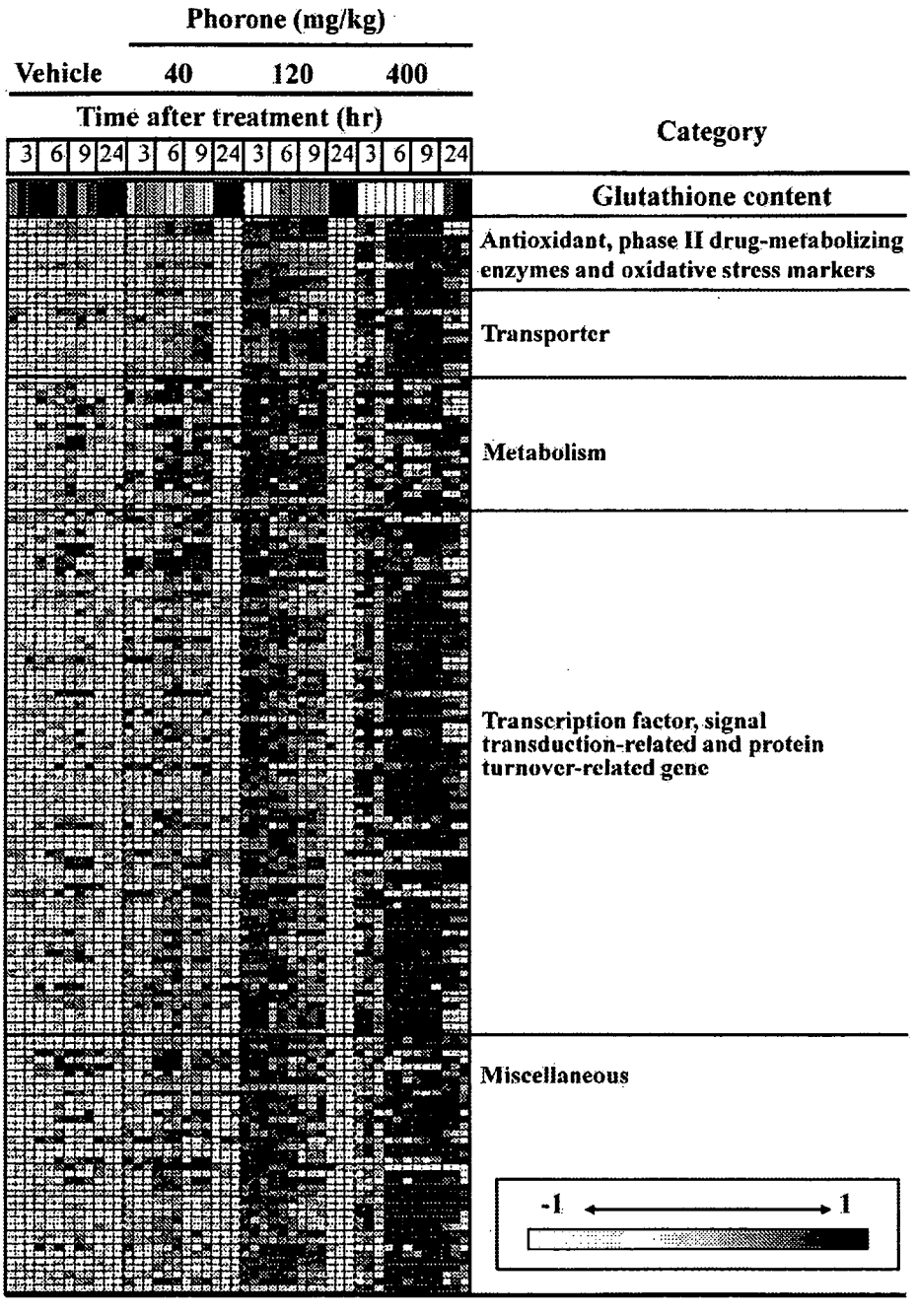

Fig. 3. Heat map representing glutathione content and gene expression level in rat liver treated with phorone.
Glutathione content and GeneChip signal data for GSH probe sets, obtained from rat livers treated with phorone or vehicle, are transformed to z-score by row, and are presented as a heat map where low and high scores are colored in white and black, respectively. Each row represents a probe set, and the vertical order of the probe sets is the same as that presented in Table 1. Each column represents individual rats treated either with phorone or vehicle.